Supporting Information

Zhang et al. 10.1073/pnas.0912306107

SI Materials and Methods

Chemical Synthesis of Azidohomoalanine. All chemicals were obtained either from Sigma-Aldrich, MP Biomedicals, Alfa Aesar, TCI, Fluka, or Acros and were used as received unless otherwise noted. The silica gel used in flash column chromatography was Fisher S704 (60-200 Mesh, chromatographic grade). Analytical TLC was conducted on Merck silica gel plates with fluorescent indicator on glass (5–20 μm, 60 Å) with detection by ceric ammonium molybdate, basic $KMnO_4$, or UV light. The ^1H and ^{13}C NMR spectra were obtained on a Bruker AVANCE-600 spectrometer equipped with a cryoprobe. Chemical shifts were reported in δ parts per million values and *J*-values were reported in Hz. MALDI-TOF mass spectra were obtained on an Applied Biosystems Voyager-DE. Fatty-acid chemical reporters (az-12, az-15, alk-12, and alk-16) (1) and clickable fluorescent detection tags (2) were synthesized in our laboratory, as previously described. Literature procedures were followed for synthesis of the precursors imidazole-1-sulfonyl azide hydrochloride (3).

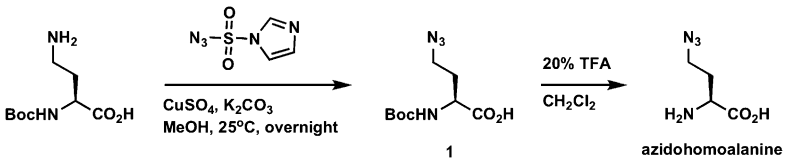

(*S*)-2-Amino-4-Azidobutanoic Acid (Azidohomoalanine). The diazo-transfer reagent, imidazole-1-sulfonyl azide hydrochloride (3) (1.0 g, 5 mmol, 1.1 equvi.) was added to a stirred suspension of commercially available Boc-Dab-OH (1.0 g, 4.6 mmol, 1 equvi.), potassium carbonate (1.17 g, 8.5 mmol), and copper (II) sulfate pentahydrate (11 mg, 46 μmol, 1 mol %) in methanol (25 mL). Upon completion of the reaction (TLC) after overnight reaction at room temperature, the mixture was concentrated and diluted in 100 mL of ethyl acetate. The organic phase was washed with 1% HCl (100 mL) twice and water (100 mL) once, followed by drying in sodium sulfate. Flash chromatography with 3:1 (hexanes: ethyl acetate) (R_f= 0.4) furnished compound 1. The identity and purity of compound 1 was checked with MALDI-TOF mass spectrometry and ^1H NMR. The combined organic fractions were further treated with 20% TFA in dry dichloromethane (20 mL) for 4 h at room temperature. Upon completion of the reaction (TLC), TFA was evaporated at reduced pressure and azeotroped with toluene (5 mL) three times. Product was redissolved in 10 mL of deionized water and lyophilized to furnish azidohomoalanine as white powder (541 mg, 82% overall yield in two steps). ^1H NMR (600 MHz, D_2O): δ = 4.15 (t, ^1H, *J* = 6.3 Hz), 3.60 (m, 2H), 2.26–2.12 (m, 2H). ^{13}C-NMR (125 MHz, D_2O): δ = 173.1, 52.3, 47.7, 29.7; MALDI-TOF: calcd. for $C_4H_9N_4O_2$ $[M+H]^+$ 145.06, found 145.13. Data were similar to previously reported synthesis of azidohomoalanine (4).

1. Charron G, et al. (2009) Robust fluorescent detection of protein fatty-acylation with chemical reporters. *J Am Chem Soc* 131:4967–4975.
2. Tsou LK, Zhang MM, Hang HC (2009) Clickable fluorescent dyes for multimodal bioorthogonal imaging. *Org Biomol Chem* 7:5055–5058.
3. Goddard-Borger ED, Stick RV (2007) An efficient, inexpensive, and shelf-stable diazotransfer reagent: imidazole-1-sulfonyl azide hydrochloride. *Org Lett* 9:3797–3800.
4. Link AJ, Vink MK, Tirrell DA (2007) Preparation of the functionalizable methionine surrogate azidohomoalanine via copper-catalyzed diazo transfer. *Nat Protoc* 2:1879–1883.

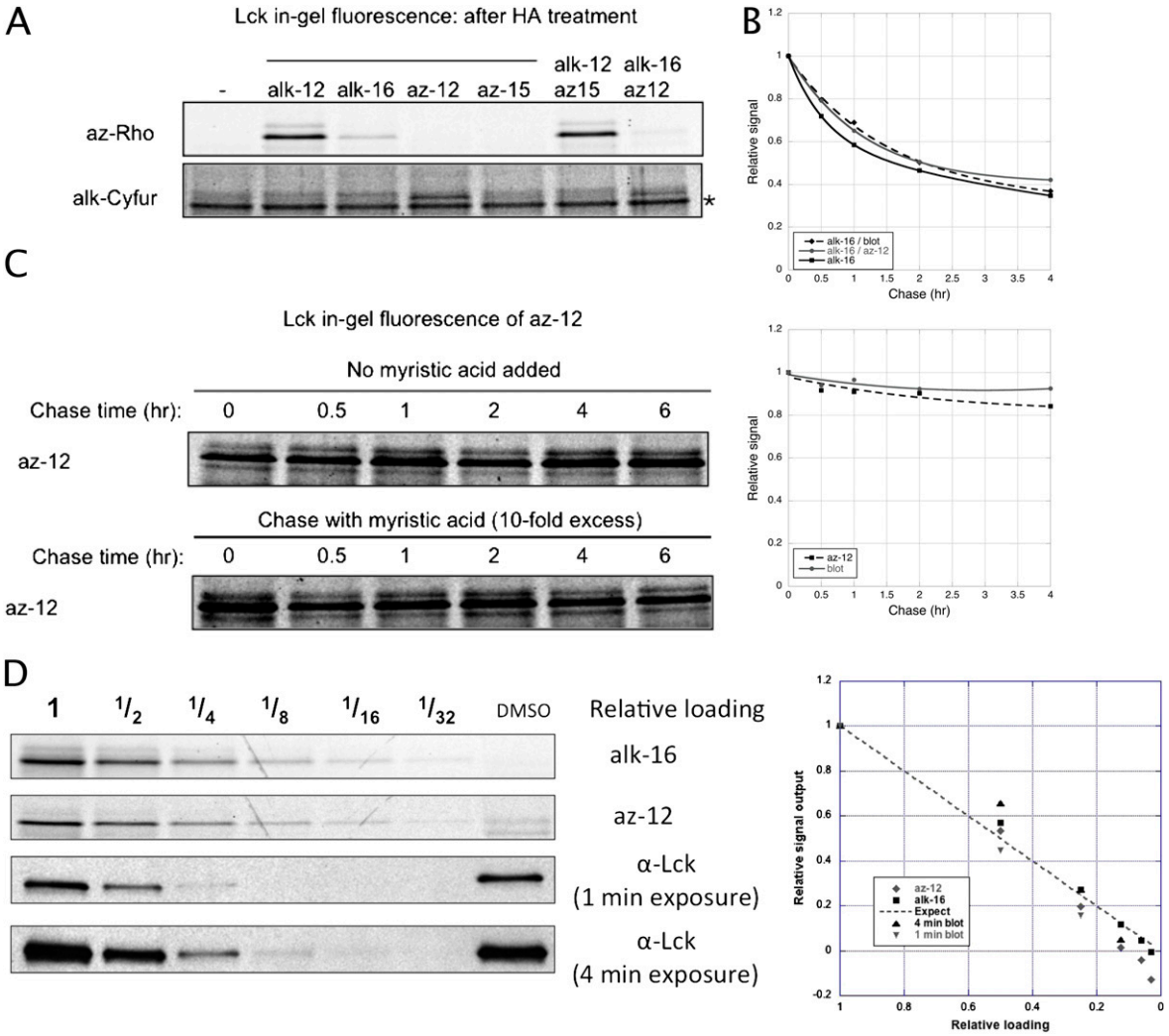

Fig. S1. Orthogonal and quantitative detection of distinct chemical reporters on Lck. (*A*) In-gel fluorescence scanning of az-12- and alk-16-modified Lck after hydroxylamine treatment. (*B*) Plots of relative signals for alk-16, az-12 fluorescence and anti-Lck blot intensities in the pulse-chase experiments. (*C*) In-gel fluorescence scanning in the alk-CyFur channel shows no significant turnover of az-12 on Lck upon chasing in the presence of excess myristate. (*D*) The range of fluorescent intensities seen in the gel is linear compared with the amount of labeled substrate. *, nonspecific bands.

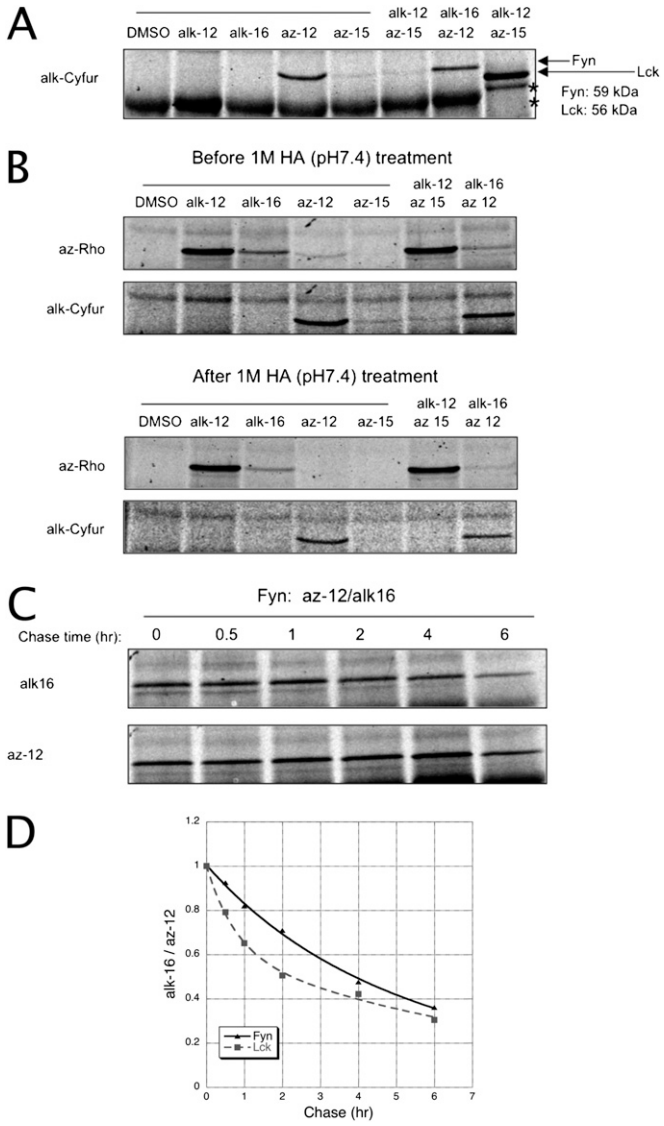

Fig. S2. Tandem fluorescence imaging of palmitate cycling on Fyn. (*A*) In-gel fluorescence scanning in the alk-Cyfur channel allows detection of az-12 on Fyn at the expected molecular weight compared with Lck. (*B*) In-gel fluorescence scanning of Fyn pre- and post- hydroxylamine treatment. (*C*) Pulse-chase analysis of Fyn. (*D*) Analysis of palmitate $t_{1/2}$ on Fyn relative to that of Lck. *, nonspecific bands.

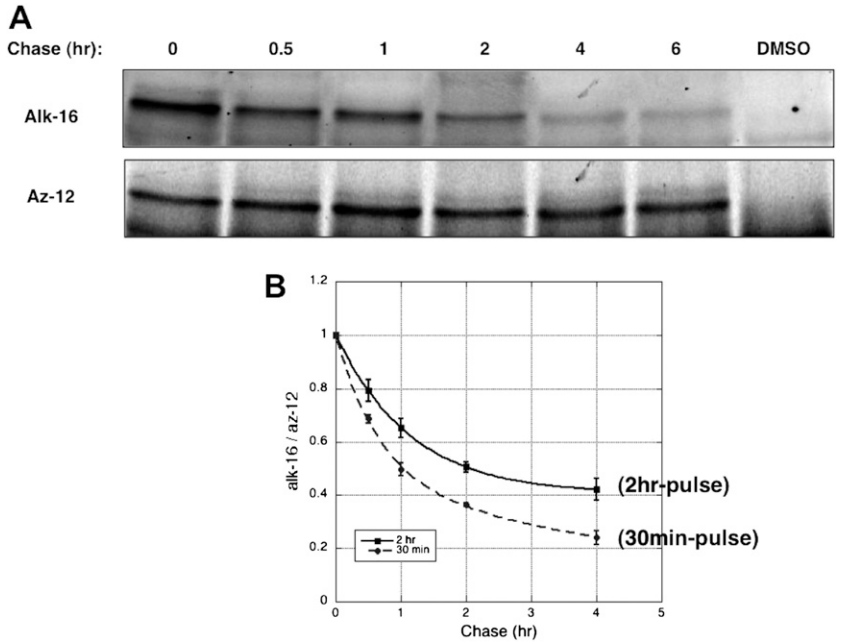

Fig. S3. Effect of long and short pulse times on calculated palmitate cycling rates. (*A*) Pulse-chase analysis of Lck with 30-min pulse time. (*B*) Normalized alk-16 to az-12 data from pulse-chase experiments comparing long and short pulse times.

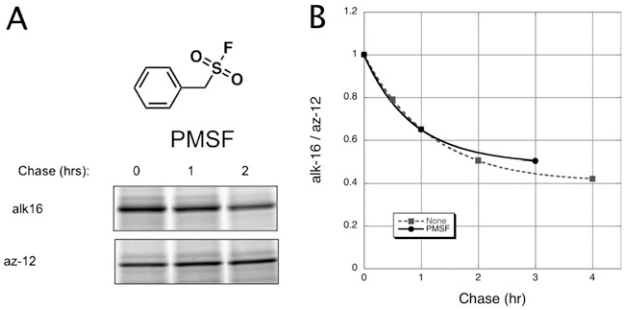

Fig. S4. PMSF does not affect palmitate turnover on Lck. (*A*) Pulse-chase analysis of Lck in the presence of phenylmethylsulfonyl fluoride. (*B*) Data from pulse-chase experiment after normalizing alk-16 to az-12 signals compared with chase conditions without chemical inhibitors.

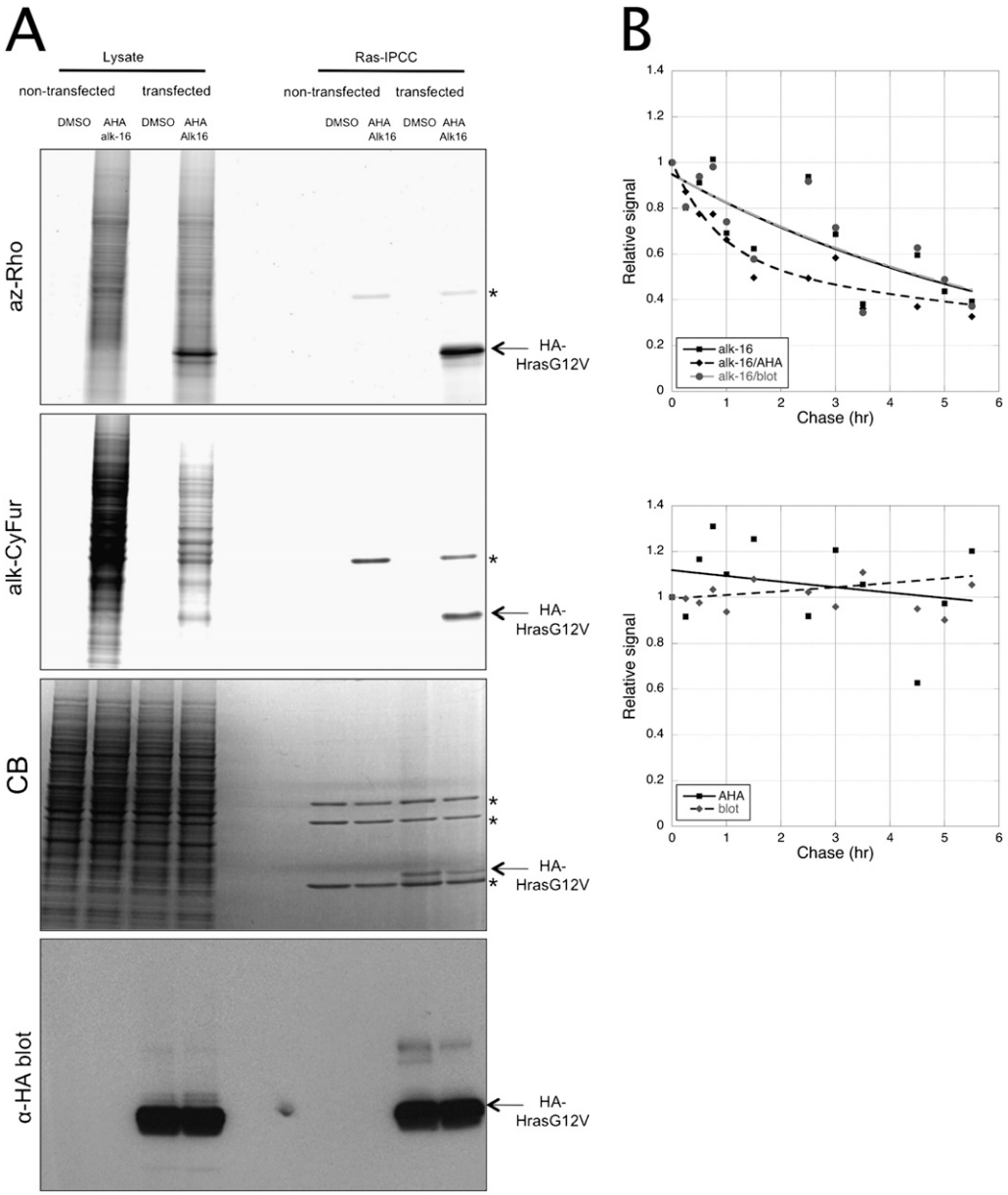

Fig. S5. Orthogonal incorporation and detection of azidohomoalanine and alk-16 on H-Ras^{G12V}. (*A*) In-gel fluorescence, coomassie blue (CB) and Western blot analyses of cellular lysates and immunopurification of dual labeling of H-Ras^{G12V} with azidohomoalanine and alk-16. (*B*) Plots of relative signals for alk-16, azidohomoalanine fluorescence, and anti-HA blot intensities in the pulse-chase experiments. *, nonspecific bands.